doi:10.14311/ppt.2017.3.245
Plasma Physics and Technology **4**(3):245–248, 2017

DEVELOPMENT OF AN EXPERIMENTAL APPROACH FOR DETERMINING THE ARC QUENCHING CAPABILITY OF DIFFERENT GASES

M. Ksoll[a,*], M. Bendig[a], P. G. Nikolic[b], A. Schnettler[a]

[a] *Institute for High Voltage Technology, RWTH Aachen University, Schinkelstr. 2, 52056 Aachen, Germany*
[b] *Siemens AG, Corporate Technology, Günther-Scharowsky-Str. 1, 91058 Erlangen, Germany*
[*] ksoll@ifht.rwth-aachen.de

Abstract. After being in the focus of sciences' and industry's research and development activities for many years, the investigation of possible SF_6 (sulfur hexafluoride) gas-alternatives has been even more intensified after the revision of the European regulation on fluorinated gases in 2014. This contribution focuses on the scientific assessment of the technical performance of several SF_6 gas-alternatives – gases and gas mixtures – currently under discussion. Therefore, a reference experimental setup, that allows the determination of the arc quenching capability of different gases as well as the axial resistance distribution of the switching arc around current zero crossing, is developed. Additionally, first experimental results for the thermal interruption capability and the arc resistance distribution of SF_6 and possible SF_6 gas-alternatives are shown.

Keywords: arc quenching capability, SF_6 gas-alternatives, arc resistance distribution.

1. Introduction

Nowadays sulfur hexafluoride (SF_6) is the state-of-the-art filling gas used in gas-insulated switchgear. Due to its outstanding characteristics, like high dielectric strength (in consequence of its high electronegativity and low average free path length) and high thermal conductivity [1], it provides both, a high arc quenching and insulation capability. On the other hand SF_6 is a potent greenhouse gas with a global warming potential of 22800 carbon dioxide (CO_2) mass equivalents [2]. At the same time optimization of today's circuit breaker technologies as well as the development of new current interruption concepts require a deep understanding of the physical processes during the switching operation, which strongly depends on the properties of the used arc quenching and insulating gas. This includes the interaction between the insulation and quenching gas and the switching arc, in particular around current zero. Especially with regard to the discussion about potential SF_6 gas-alternatives, a technical evaluation of the arc quenching capability of alternative arc quenching and insulating gases under comparable boundary conditions is necessary. Ongoing research activities identified CO_2 [3] and air [4] as candidates for natural SF_6 alternatives. Additionally to these two, nitrogen (N_2) as well as gas mixtures with fluorinated compounds will be examined in this work.

To gain a better understanding of the quenching behavior of the different gases, an experimental setup is developed, which allows the characterization of the thermal arc quenching performance in a reference circuit breaker model. In order to investigate the effectiveness of different cooling mechanisms in different gases, a minimal-intrusive measurement method is applied. It is based on capacitive field probes and delivers measurement data for the arc potential drop and thereby the spatial resistance distribution of the switching arc in the vicinity of current zero.

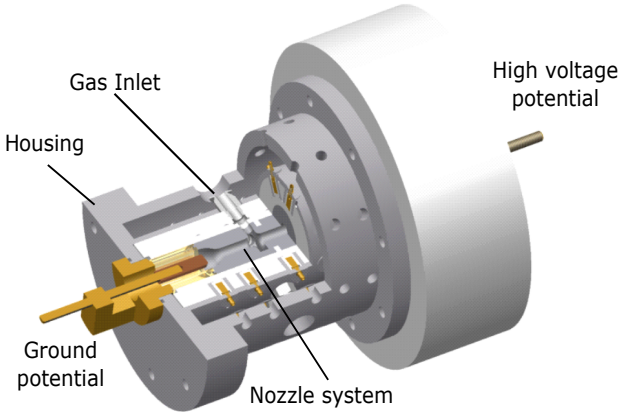

Figure 1. Cross-sectional view of the reference circuit breaker model for the characterization of the arc quenching capability.

2. Experimental Setup

For the determination of the thermal arc quenching capability a reference circuit breaker model is developed (cf. Figure 1). To minimize the influence of variable parameters caused by moving contacts, the tungsten-copper electrodes are fixed and the switching arc is initiated by an ignition wire. The two electrically isolated housing parts of the model are connected to high voltage and ground potential respectively. The blowing of the arc is realized by a gas

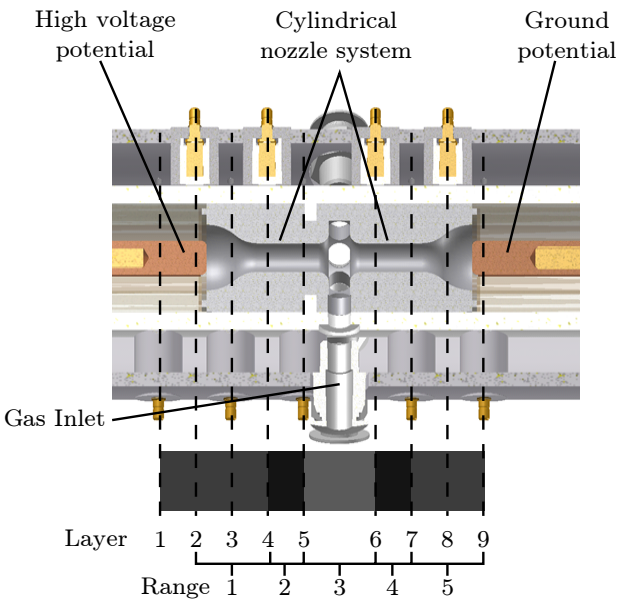

Figure 2. Distribution of the capacitive field probes.

flow from an external pressure tank with a volume of $V = 20\,\mathrm{l}$ through nine radially distributed openings in the center of the insulation nozzle. Therefore different blowing pressures can be investigated independently of the current. The radial blowing leads to a formation of a stagnation point in the nozzle center and consequently an axial gas flow through the arcing zone towards the electrodes.

Multiple capacitive field sensors placed around the nozzle measure the displacement current and thus the potential drop along the switching arc. These sensors are distributed in nine layers along the cylindrical axes (cf. Figure 2). On each layer three sensors are arranged at an angle of 120 degrees to enable the determination of the position of the arc inside the nozzle by the use of triangulation. Additionally, a fourth sensor is placed in each layer to determine the arc radius [5]. All 36 signals are amplified and converted into optical signals to be transferred to the measurement system via optical transmission paths. The measurement is carried out using a multi-channel transient recorder. The different layers are assigned to five areas, the diffusor and nozzle throat (on each side) and the stagnation point respectively (cf. Table 1). With this classification a comparison of the significant nozzle areas, where different cooling mechanisms are expected, is possible.

If the arc is assumed to be a conductive cylinder centered in the nozzle, the arc potential leads to a radial electric field E_r towards the grounded housing and therefore towards the sensors (cf. Figure 3). Thus the current density

$$J_r = \sigma \cdot E_r + \epsilon \frac{\mathrm{d}E_r}{\mathrm{d}t} \tag{1}$$

is induced into the sensors surface A. The sensor is connected to ground potential via a termination load Z. The resulting current through the load is

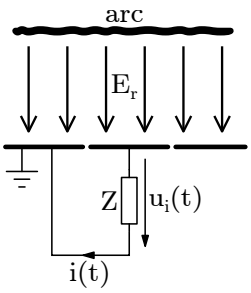

Figure 3. Working principle of a capacitive field sensor.

$i = \int_A J_r \,\mathrm{d}A$. The load Z, which is a parallel connection of the stray capacitance C_s between sensor plate and shield and a defined resistor R, is dimensioned in a way that the measurement system is overcompensated:

$$RC_s \ll \frac{\sigma}{\epsilon} \tag{2}$$

The resulting voltage measured at the resistance of a certain sensor $u_i(t)$ is proportional to the derivation of the electric field on this sensors surface [5]:

$$u_i(t) = \epsilon\, A\, R\, \dot{E}_r(t) \tag{3}$$

As the the radial electric field E_r is proportional to the arc voltage, the arc potential $\Phi_{\mathrm{arc},i}$ near the sensor can be calculated by

$$\Phi_{\mathrm{arc},i} = \Psi i \cdot \int_t u_i(t)\,\mathrm{d}t - \Phi_{\mathrm{el}} \cdot \Psi_{\mathrm{el},i} \tag{4}$$

with Ψ_i being the coupling factor between arc and sensor i and $\Psi_{\mathrm{el},i}$ being the coupling factor between the electrode and the sensor i. To determine the coupling factors for each sensor, a metallic rod covering the whole nozzle length is inserted into the nozzle. A sinusoidal voltage is applied to the rod and the signals of the sensors are analyzed by taking the ratio of the original rod voltage and the coupled voltage signal. With this method the coupling between arc and sensors is determined. For the determination of the coupling factors $\Psi_{\mathrm{el},i}$ the rod is replaced by a rod with electrodes at its ends and the factors are calculated (cf. Figure 4). The coupling factors Ψ_i are now subtracted to obtain the coupling of the electrodes without the rod. The spatial resistance distribution, which is equal to the relative voltage distribution, is calculated by subtracting the arc potential of adjacent layers and normalizing it to the potential of layer 1.

The total resistance is obtained from an external current and voltage measurement using a Rogowski current transducer and a high voltage probe. A first validation shows, that the measuring method is able to detect the influence of turbulent and laminar flow sections [6]. The reference circuit breaker model is located inside a test vessel filled with the blowing gas at ambient pressure. To prevent the measurement of displacement currents, the ground potential of the electrode is isolated from the ground potential of the vessel. For an easy maintenance and change of the

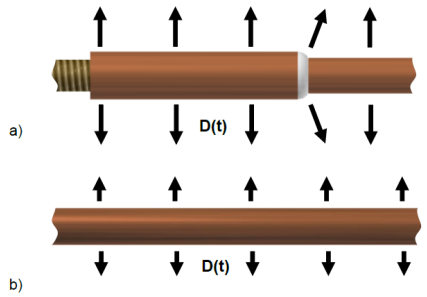

Figure 4. Metallic rods - with (a) and without (b) electrode - for the determination of the coupling factors and the influence of the electrodes.

Range No.	Layer	Area of nozzle
1	2,3,4	Diffusor
2	4,5	Nozzle Throat
3	5,6	Stagnation Point
4	6,7	Nozzle Throat
5	7,8,9	Diffusor

Table 1. Classification of measurement signals in five ranges.

ignition wire, the reference model is assembled on a guide rail system (cf. Figure 5). A gas panel connects the external pressure tank to the nine pneumatic hoses establishing the blow gas flow. In addition, a measurement of the static blowing pressure is possible in the gas panel.

In order to emulate multiple current zero crossings, the high voltage part of the Weil-Dobke circuit, a simple LC resonant circuit with a frequency of $f = 955\,\mathrm{Hz}$, is used for current injection. This has the advantage, that high current steepnesses can be obtained with relatively low current amplitudes. Due to the damping of the circuit, the current steepness decreases with an increasing number of current zero crossings. Consequently, multiple current zero crossings can occur in one test. As the current amplitude provided by the test circuit exponentially decays with each oscillation the current steepness at the current zero crossing decreases accordingly.

At the beginning of an experiment the blowing is initialized by a magnetic valve. The spark gap in the test circuit is triggered when the static blowing pressure reaches its maximum. Due to the low pressure drop in the arcing phase – even when multiple current zero crossings occur – the blowing pressure is not significantly changing during the test.

3. Results and Discussion

In Figure 6 the first measurement results for the thermal interruption capability of gas mixtures (CO_2 with fluoroketone and fluoronitrile), CO_2, air and N_2 are shown in comparison to SF_6. The interruption capability of each gas is characterized by the thermal

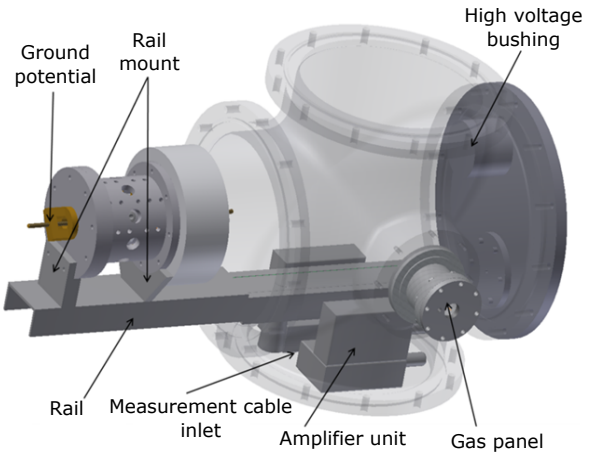

Figure 5. Construction of the test vessel.

interruption limit $\mathrm{d}i/\mathrm{d}t_{limit}$:

$$\left(\frac{\mathrm{d}i}{\mathrm{d}t}\right)_{\text{limit}} = \frac{1}{k}\cdot\sum_{n=1}^{k}\left[\left(\frac{\mathrm{d}i}{\mathrm{d}t}\right)_{n}\cdot\left(\frac{R_{200,n}}{R_{\text{crit}}}\right)^{\frac{1}{m}}\right], \quad (5)$$

with k being the number of current zero crossings tested. The arc resistance at exact current zero crossing cannot be obtained numerically. Therefore the resistance R_{200} at $t = -200\,\mu\mathrm{s}$ before current zero crossing is used. The critical current steepness is exponentially depending on R_{200} [7], hence the exponent m can be derived from a curve fitting through all measured points. The resistance R_{crit} is calculated as the mean value between the highest R_{200} of a failed interruption and the lowest R_{200} of a successful interruption.

Figure 6a shows the results for a blowing pressure $p_{\text{abs}} = 0.15\,\mathrm{MPa}$, which is in the typical range for medium voltage applications, while Figure 6b shows the results for $p_{\text{abs}} = 0.65\,\mathrm{MPa}$, which is in the typical range for high voltage applications. Air and N_2 show a significantly reduced thermal interruption capability in the range of 46 % to 54 % compared to SF_6. CO_2 reaches a thermal interruption capability above 80 % compared to SF_6. The thermal interruption capability of the fluorinated gas mixtures is in the range of 83% to 87% for $p_{\text{abs}} = 0.65\,\mathrm{MPa}$ and shows a decreased value of 71% for $p_{\text{abs}} = 0.15\,\mathrm{MPa}$. Overall, there is no significant increase in the thermal interruption capability achieved by adding the specific fluorinated components to the gas.

An example for a resistance distribution of a successful switching operation in CO_2 with a blowing pressure of $p_{\text{abs}} = 1.1\,\mathrm{MPa}$ is shown in Figure 7 for $t = \pm 10\,\mu\mathrm{s}$ around current zero. The relative resistance of the area around the stagnation point is significantly increasing around current zero.

Due to the decreasing arc radius near current zero, an increased turbulent eddy formation affecting the remaining arc channel in the stagnation point area is expected to occur. Thus it is assumed, that next to convective cooling effects the success of this switching

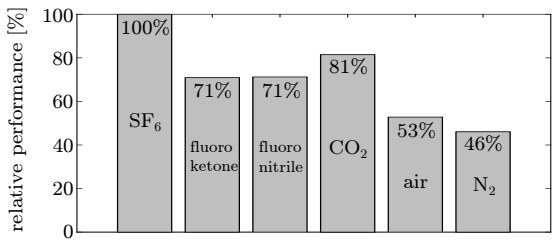

(a) $p_{\mathrm{abs}} = 0.15\,\mathrm{MPa}$

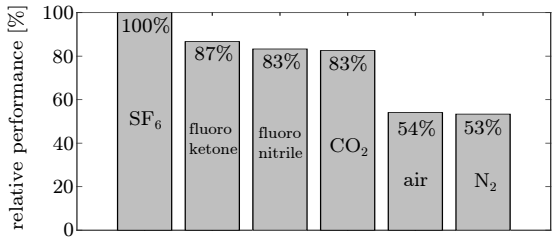

(b) $p_{\mathrm{abs}} = 0.65\,\mathrm{MPa}$

Figure 6. Comparison of the thermal arc interruption performance of gas mixtures (CO_2 with fluoroketone and fluoronitrile), CO_2, N_2 and air related to SF_6 for different blow gas pressures

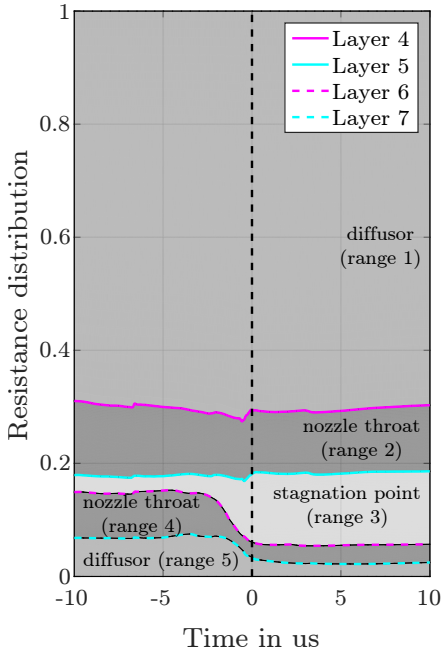

Figure 7. Resistance distribution for a successful arc quenching with CO_2 for blow gas pressure $p_{abs} = 1.1$ MPa.

operation is also dependent on this strong turbulent cooling around the stagnation point. The high relative resistance of the diffusor range at the high voltage electrode (range 1) is assumed to be a consequence of a deviation between the determined coupling factor and the actual coupling due to arc looping or multiple arcing base points.

4. Conclusion

A test setup for experimental investigations of the thermal interruption capability of SF_6 gas-alternatives was developed. Additionally, a minimal-intrusive measurement method to determine the resistance distribution of the switching arc is used. Thus, the effectiveness of different cooling mechanisms for different gases can be examined. This leads to a better understanding of the current interruption processes in different gases to identify possible SF_6 gas-alternatives. First measurements were performed with SF_6, gas mixtures (CO_2 with fluoroketone and fluoronitrile), CO_2, N_2 and air at different blowing pressures to validate the test setup. In this setup the thermal interruption capability of CO_2 is less than 20 % lower than SF_6 for both blowing pressures. For the fluorinated gas mixtures no significant improve of the thermal interruption capability is observed. For low blowing pressures the thermal interruption capability of these gas mixtures is even lower than for CO_2.

A determination of the position as well as the radius of the arc is possible but has not been conducted yet. For a validation, further research is necessary. Additionally the influence of the higher frequency test current, and therefore the lower current amplitude and lower heating of the arcing zone has to be determined in future examinations.

References

[1] M. Kriegel. Einfluss des Düsenmaterials auf das Ausschaltverhalten von SF_6–Selbstblasschaltern. *Ph.D. Thesis, Institute for High Voltage Technology, RWTH Aachen University*, 1999.

[2] UNFCCC. Kyoto protocol to the united nations framework convention on climate change. *Framework Convention on Climate Change*, 1997. `http://unfccc.int/resource/docs/convkp/kpeng.pdf`.

[3] T. Uchii et al. Fundamental research on SF_6–free gas insulated switchgear adopting CO_2 gas and its mixtures. In *Proc. of Internat. Sym. on EcoTopia Science*, 2007. `http://www.esi.nagoya-u.ac.jp/h/isets07/Contents/Session04/1333Uchii.pdf`.

[4] P.C. P. C. Stoller et al. CO_2 as an arc interruprion medium in gas circuit breakers. In *IEEE Trans. on Plasma Sci.*, volume 41, pages 2359–2369, 08 2013. `doi:10.1109/TPS.2013.2259183`.

[5] M. Hoffacker. Verfahren zur ortsaufgelösten Messung der Widerstandsverteilung eines axial beblasenen Schaltlichtbogens. *Ph.D. Thesis, Institute for High Voltage Technology, RWTH Aachen University*, 2012.

[6] M. Weuffel, P. G. Nikolic, and A. Schnettler. Investigations on the spatial arc resistance distribution of an axially blown switching arc. *Proc. 20th Int. Conf. on Gas Discharges and their Applications, Orleans, France*, 2014.

[7] C. M. Franck, M. Claessens, and H. Nordborg et al. Thermal interruption behaviour of high-voltage circuit breakers. *Proc. 15th Int. Conf. on Gas Discharges and their Applications, Toulouse*, 2004.